



# Environmental impact of the launch vehicle “Soyuz-FG” emergency falling in Kazakhstan

Ivan Semenkov<sup>1</sup> · Erlan Bekeshev<sup>2,3</sup> · Yelena Stepanova<sup>2</sup> · Andrey Karpachevskiy<sup>1</sup> · Sergey Lednev<sup>1</sup> · Galina Klink<sup>4</sup> · Yerasyr Yerzhanov<sup>2</sup> · Akylbek Bapyshev<sup>2</sup> · Tatyana Koroleva<sup>1</sup>

Received: 9 May 2024 / Accepted: 2 January 2025

© The Author(s), under exclusive licence to Springer-Verlag GmbH Germany, part of Springer Nature 2025

## Abstract

On October 11, 2018, in the Ulytau region of the Republic of Kazakhstan, the Soyuz-FG launch vehicle carrying a crewed MS-10 spacecraft failed. It resulted in the release into the fragile arid ecosystems of rocket propellants, i.e., jet fuel of toxic hazard class 4 and carcinogenic unsymmetrical dimethyl hydrazine (heptyl, UDMH). In this paper, we described the results of soil surveys conducted in 2018, 2019, 2022, and 2023. In the fragile arid ecosystems in Central Kazakhstan, due to the emergency falling of the launch vehicle, environmental consequences were registered at a total area of about 1350 m<sup>2</sup>, including spillage of jet fuel and UDMH in the territories of 400 m<sup>2</sup> and 9 m<sup>2</sup>, respectively. The third stage disintegrated and fell down within an area of 4.4 km<sup>2</sup>. Immediately after the emergency crash of the second stage, the content of total petroleum hydrocarbons (TPHs) reached 1645 mg/kg, decreasing 10 times in 3.5 years. At the fuel tank falling site, the concentration of highly toxic carcinogenic UDMH and nitrosodimethylamine (NDMA) reached 22 and 9 mg/kg, which is many times higher than the maximum permissible concentrations. Four years after reclamation, the content of both substances did not exceed 0.05 mg/kg—the lower limit of sensitivity of a highly performed liquid chromatography. The content of TPHs, water-soluble Cl<sup>-</sup> and SO<sub>4</sub><sup>2-</sup>, and alkalinity from CO<sub>3</sub><sup>2-</sup> was significantly ( $p < 0.05$ ) higher in autumn of 2022, and the content of total N, water-soluble NO<sub>3</sub><sup>-</sup> and NO<sub>2</sub><sup>-</sup>, and alkalinity from HCO<sub>3</sub><sup>-</sup> was higher in spring of 2023. In spring and autumn, the content of exchangeable Ca<sup>2+</sup> and Mg<sup>2+</sup>, cation exchange capacity was similar ( $p > 0.05$ ). The presented materials can be used to optimize the restoration of disturbed arid ecosystems and future monitoring work at sites of regular landing of the first stages and emergency crash sites of launch vehicles.

**Keywords** Environmental impact · Nitrogen · Remediation · Rocket propellant components · Ecological consequences · Ecological damage · Carcinogenic chemicals

## Introduction

Space rockets like all other powered vehicles affect the environment at all stages of their use (Dallas et al. 2020; Liu et al. 2022; Koroleva et al. 2024). In the Baikonur cosmodrome, using of the Proton and Soyuz launch vehicles is associated with environmental impact on the fragile arid ecosystems. In 1999–2024, using of the Soyuz launch vehicles was accompanied by predominantly allowable ecological consequences (Epifanov et al. 2009; Maksimenko 2020). However, there are several speculative works postulating the formation of environmental disaster zones as a result of the use of the Baikonur cosmodrome without any reliable and reproducing data (UNDP 2004; Williams 2013; Kopack 2019, 2021; Dallas et al. 2020). The only accident involving a launch vehicle Soyuz

---

Responsible Editor: Philippe Garrigues

✉ Ivan Semenkov  
semenkov@geogr.msu.ru

- <sup>1</sup> Lomonosov Moscow State University, Moscow, Russia
- <sup>2</sup> Branch Office of the Republican State Enterprise “Infracos”, Almaty, Kazakhstan
- <sup>3</sup> Almaty University of Power Engineering and Telecommunications named after G.Daukeev, Almaty, Kazakhstan
- <sup>4</sup> National Research University Higher School of Economics, Moscow, Russia

occurred on 11.10.2018 (Koroleva et al. 2021). But its environment was analyzed insufficiently (Bekeshev et al. 2024).

Due to the first stage being separated irregularly, the linked second and third stages fell to the ground accidentally. The landing module holding the cosmonauts separated normally and the astronauts received only significant overloads. The first stage landed in the specially designated drop area. Fragments of the second stage and the fairing crash-landed in an unspecified territory of other falling regions. The third stage disintegrated into at least 65 fragments and fell east of the falling region in the Kara-Kengir River valley (at least 65 m from it) within an area of 4.4 km<sup>2</sup>. Four fragments of the tail compartments were found 7 km south of the area where the third-stage fragments were released. Spherical fuel tanks of the crewed spacecraft Soyuz MS-10 with highly toxic unsymmetrical dimethylhydrazine (UDMH or heptyl) landed on the northern border of the area where fragments of the third stage were dispersed, 0.9 km from the Kara Kengir River.

Traditionally, among all kinds of aerospace transportation impact, the greatest public attention has been attracted to environmental pollution with highly toxic carcinogenic rocket propellants namely UDMH. At the falling site of fairing, due to the absence of contamination of ecosystems by rocket propellants (based on the results of the environmental impact assessment in October 2018), subsequent monitoring of soil properties was not initiated. The fall of the blocks of the first stage of the Soyuz launch vehicle was accompanied by the allowable entry of jet fuel and H<sub>2</sub>O<sub>2</sub> into the arid ecosystems. Soil polluted with highly toxic UDMH was transported to the Baikonur cosmodrome for remediation, similar to the previous accident of the Proton launch vehicle, which was also accompanied by UDMH entering ecosystems.

To assess the long-term consequences for the ecosystems in Central Kazakhstan of the emergency fall of fragments of the Soyuz-FG launch vehicle launched on October 11, 2018, and to control morphological and chemical properties of the soils in the affected areas in September 2022 and in May 2023, an international group of Kazakh and Russian researchers was created. The purpose of these works was to assess the current state of ecosystems, including soils according to chemical properties.

In total, three areas were examined, corresponding to emergency falling sites of the second stage of the Soyuz-FG launch vehicle, spherical fuel tanks of the Soyuz-MS-10 spacecraft, and background areas. Depending on the pollutants at each site, the most relevant analytes were selected from the list of those controlled in the Republic of Kazakhstan at the falling regions of the first stage of the Proton and Soyuz launch vehicles. Moreover, preliminary field works were conducted in 2018 and 2019.

## Materials and methods

The main field soil works were carried out in September 2022 and May 2023 and included a description of three soil cross-sections and soil sampling (Table 1). In addition, an initial environmental assessment was carried out as part of the route planning process after each launch, and preliminary fieldwork was conducted 1 year after the accident, respectively. From the cross-sections, soil samples were taken from each genetic horizon (from the surface to a depth of 110 cm). At the second stage falling site, samples were taken from the auger holes at depths of 0–25 and 25–50 cm. At the falling site of spherical fuel tanks and in background areas outside the impact zone resulting from accident-related

**Table 1** Brief characteristics of the studied areas

Characteristic	Second stage falling site	Falling site of the spherical fuel tanks	Background area
Coordinates	N 47° 27'55.2" E 67° 47' 52.7"	N 47° 31' 30.6" E 67° 58' 42.5"	N 47° 35' 24.6" E 67° 49' 05.4"
Relief	Leveled surface at the interfluvium	An elongated local micro depression associated with the floodplain of the Kara Kengir River	
Vegetation	Grassy and ephemeral vegetation with predominance of <i>Stipa sareptana</i> and <i>Cerastium arvense</i>	Shrubby vegetation with predominance of <i>Artemisia pauciflora</i> and <i>Atriplex cana</i>	Shrubby vegetation with predominance of <i>Anabasis salsa</i> and <i>Atriplex cana</i>
Total projective cover of vegetation, %	40–50	20–30	20–30
Soil name	Calcic Solonetz (Endorenic, Anoclayic, Epic, Endoskeletal)	Calcic Gypsisols (Endic, Siltic)	Calcic Gypsisols (Clayic, Endic)
Soil horizon name	E <sub>8</sub> –Bt <sub>n25</sub> –Bk <sub>135</sub> –Bk <sub>266</sub> –2Ck <sub>90</sub>	Ak <sub>8</sub> –ABk <sub>19</sub> –Bwy <sub>70</sub> –Cy <sub>110</sub>	Ak <sub>5</sub> –ABk <sub>20</sub> –By <sub>30</sub> –Cy <sub>95</sub>
Parent material	Eluvial-deluvial loams	Ancient alluvial loams	Ancient alluvial loams

The subscript to the right of the horizon index indicates its lower boundary (in cm); for parent material, the depth of the section

factors, samples were taken from the auger holes at depths 0–50, 50–100, and 100–150 cm (Table S 1).

All soil properties were analyzed in accordance with methods approved in Russia and Kazakhstan. As this work was related to environmental impact assessment, certified methods were used that are within the scope of the accreditation of the relevant Russian and Kazakh laboratories. The focus was on indicators of substance composition that reflect soil functioning and analytes for which maximum permissible concentrations have been justified both in Russia and Kazakhstan.

The pH value, cation–anion composition, specific electrical conductivity, and mass of the dense residue were determined in the aqueous extract. Cation exchange capacity (CEC) was measured using a  $\text{BaCl}_2$  extraction solution. Basicity was determined titrimetrically with sulfuric acid and indicators namely methyl orange and phenolphthalein (Pansu and Gautheyrou 2006). The total nitrogen (N<sub>tot</sub>) and organic carbon (TOC) content was determined using the Kjeldahl and bichromate method, respectively.

The methods of extraction of UDMH and NDMA from the soil are based on extraction using 1 M hydrochloric acid, distillation with vapor into acid solution, and subsequent analysis of the distillation by ion chromatography. The content of UDMH and NDMA was determined using ion chromatography with amperometric detection (Smolenkov et al. 2005) and high-performance liquid chromatography with amperometric or spectrophotometric detection (Ponomarenko et al. 2009), respectively. Quantitative calculations were carried out using the external standard method by peak area.

TPHs were determined fluorimetrically using the spectroscopy method by Shpol'skii (Gooijer et al. 1997; Gennadiyev et al. 2015) based on the fluorescence of some unsaturated petroleum components bearing fluorophores in their structure. This simple, quick, low-cost technique provided a strong correlation with commonly used reference methods, e.g., chromatography (Patra and Mishra 2000; Meira et al. 2011; Włodarski et al. 2013; Pikovskii et al. 2017). TPHs were extracted from the soil with hexane under dynamic conditions using a 25 cm<sup>3</sup> glass volumetric flask and “red ribbon” filters, pre-washed with hexane, and tested for residual concentration of TPHs. TPH concentration was measured on a Fluorat-02 liquid analyzer (Russia) using hexane-based calibration solutions. The rocket propellant differs from other hydrocarbon fuels by the low content of unsaturated compounds and consists of mainly cycloalkanes not capable of fluorescing. This may result in significant underestimation of the measured TPH values. However, the fluorimetric determination of TPHs in soils is one of the certified methods in both Russia and the Republic of Kazakhstan, unlike, for example, the chromatographic determination of kerosene. The corresponding method (Bolotnik et al.

2015, 2018) is certified only in Russia and therefore cannot be used in such arbitration issues as assessment of soil pollution with hydrocarbons in the Republic of Kazakhstan.

Subsets were used for subsequent calculations and analyses—descriptive statistics to characterize the relevant area and its parts, paired Wilcoxon test to assess the influence of the seasonality factor on the controlled properties, Spearman correlation coefficients, Mann–Whitney *U*-test. The specified calculations and visualization of the results were conducted using Excel, Statistica-7 packages, and Arc-Gis-10 software. The threshold level for identifying significant differences was taken to be  $p = 0.05$ .

## Results and discussion

Due to the emergency falling the launch vehicle, the ecosystems of three sites in the Kazakh Upland (Ulytau region, Central Kazakhstan) were subjected to mechanical, chemical, and pyrogenic effects, typical for the rocket and space transportation (Koroleva et al. 2023) at a total area of about 1350 m<sup>2</sup>, including spillage of jet-fuel at the second stage falling site and spillage of UDMH from the spherical fuel tanks in the territories of 400 m<sup>2</sup> and 9 m<sup>2</sup>, respectively. At the latter spillage site, polluted soil was removed for subsequent remediation in the Baikonur cosmodrome. Pyrogenic impact zones covered a total area of about 950 m<sup>2</sup> at the fuel tank falling site.

As data on the pH value and the content of TPHs obtained by two laboratories are in good agreement with each other, further in the text, visualization of material obtained in one of the laboratories is presented. Data obtained by the Yuzhny Space Center in 2022 and 2023 are used to describe seasonal differences in the soil properties. Temporal changes in the content of rocket propellants and their derivatives, as well as pH value in the soils of two falling sites, are characterized according to the data by Infracos laboratory.

## Background area

In the background areas, the content of exchangeable  $\text{Ca}^{2+}$  and  $\text{Mg}^{2+}$  was 10–27 and 0.8–10.6 mmol/100 g, respectively, with a cation exchange capacity of 30–50 mmol/100 g (Table 2). There are no significant differences in spring and autumn data sets from three cross-sections (Table S 2). The soil pH value ranged from 8.2 to 10.2.  $\text{NO}_3^-$  content did not exceed 130 mg/kg—maximal permissible concentration. In soils,  $\text{NO}_3^-$  content did not differ significantly between spring and autumn according to the Wilcoxon paired test.

The content of water-soluble  $\text{Cl}^-$ ,  $\text{SO}_4^{2-}$ , and basicity of  $\text{CO}_3^{2-}$  is higher in autumn, and the basicity of  $\text{HCO}_3^-$  is higher in spring. This is due to the fact that by autumn, easily soluble salts with rising vertical flows from the subsoil to the

**Table 2** Chemical properties of the studied soils (data by the laboratory of the Yuzhny Space Center)

Soil property	Year	Sampling*	min	max	<i>M</i>	Me	SD	Cv, %	<i>n</i>
Background area, *sampling depth in cm									
Exchangeable Ca <sup>2+</sup> , mmol/100 g	2023	0–25	10	10	10	10	0	4	2
	2022		11	12	11	11	1	11	2
	2023	25–100	13	27	23	27	8	36	3
	2022		11	17	15	17	3	20	3
Water-soluble Cl <sup>-</sup> , mg/kg	2023	0–25	<1	77	39	39	54	140	2
	2022		798	8206	4502	4502	5238	116	2
	2023	25–100	<1				–	–	3
	2022		3741	12776	7094	4764	4948	70	3
Basicity of CO <sub>3</sub> <sup>2-</sup> , mmol/100 g	2023	0–25	0.15	0.15	0.15	0.15	–	–	2
	2022		<0.1	0.50	0.28	0.28	0.32	116	2
	2023	25–100	<0.1				–	–	3
	2022		<0.1	0.40	0.17	<0.1	0.20	121	3
Basicity of HCO <sub>3</sub> <sup>-</sup> , mmol/100 g	2023	0–25	0.52	0.88	0.70	0.70	0.25	36	2
	2022		0.30	0.65	0.48	0.48	0.25	52	2
	2023	25–100	0.50	0.55	0.52	0.50	0.03	6	3
	2022		0.20	0.55	0.37	0.35	0.18	48	3
Exchangeable Mg <sup>2+</sup> , mmol/100 g	2023	0–25	3.6	3.8	3.7	3.7	0.1	4	2
	2022		1.7	3.0	2.4	2.4	0.9	39	2
	2023	25–100	0.8	3.2	2.2	2.7	1.3	57	3
	2022		4.2	10.6	7.4	7.3	3.2	43	3
NO <sub>2</sub> <sup>-</sup> , mg/kg	2023	0–25	<1				–	–	2
	2022		<1				–	–	2
	2023	25–100	<1	8.8	2.6	0.5	4.2	161	4
	2022		<1				–	–	4
Water-soluble NO <sub>3</sub> <sup>-</sup> , mg/kg	2023	0–25	23	116	70	70	66	95	2
	2022		<1	3.9	2.2	2.2	2.4	109	2
	2023	25–100	3	130	38	10	61	162	4
	2022		<1	110	32	8	53	167	4
Water-soluble SO <sub>4</sub> <sup>2-</sup> , mg/kg	2023	0–25	<1	273	137	137	193	141	2
	2022		3221	9498	6360	6360	4439	70	2
	2023	25–100	<1				–	–	3
	2022		1624	10,447	5766	5226	4436	77	3
CEC, mmol/100 g	2023	0–25	30	32	31	31	1	5	2
	2022		28	34	31	31	4	14	2
	2023	25–100	36	50	45	50	8	18	3
	2022		36	50	45	50	8	18	3
N <sub>tot</sub> , %	2023	0–25	0.09	0.12	0.10	0.10	0.02	22	2
	2022		0.07	0.08	0.08	0.08	0.01	10	2
	2023	25–100	0.07	0.17	0.12	0.14	0.05	41	3
	2022		<0.01	0.05	0.02	0.01	0.03	133	3
pH	2023	0–25	8.2	10.2	8.9	8.7	0.8	8	6
	2022		8.7	9.6	9.0	8.8	0.5	5	6
	2023	25–100	7.7	9.1	8.4	8.3	0.5	6	10
	2022		6.2	9.6	8.7	9.1	1.0	12	10
Second stage falling site (sampling depth 0–25 cm), *sampling distance from the fragments in m									
TPH, mg/kg	2023	0–3	<5	9.4	4.8	2.5	3.2	68	5
	2023	4–5	<5				–	–	3
	2022	0–3	<5	35.0	9.0	2.5	14.5	161	5
	2022	4–5	<5	155.0	64.2	35.0	80.3	125	3
	2022	7–50	<5	5.8	<5	<5	1.2	40	8

**Table 2** (continued)

Soil property	Year	Sampling*	min	max	<i>M</i>	Me	SD	Cv, %	<i>n</i>
pH	2023	0–3	6.8	8.8	7.5	7.1	0.8	11	5
	2023	4–5	6.2	7.4	7.1	7.1	0.4	6	7
	2022	0–3	6.4	6.9	6.6	6.5	0.2	3	5
	2022	4–5	6.4	8.1	7.4	8.0	0.8	11	7
	2022	7–50	6.5	6.9	6.7	6.7	0.1	2	8
Second stage falling site (sampling depth 25–50 cm), *sampling distance from the fragments in m									
TPH, mg/kg	2023	0–3	<5	11.7	<5	<5	4.1	95	5
	2023	4–5	<5				–	–	5
	2022	0–3	<5				–	–	5
	2022	4–5	<5	28.0	11.1	<5	12.1	109	5
	2022	7–50	<5	5.8	<5	<5	1.2	40	8
pH	2023	0–3	6.6	7.8	6.9	6.7	0.5	7	5
	2023	4–5	6.4	8.8	7.9	8.0	0.8	10	9
	2022	0–3	6.3	7.4	6.6	6.5	0.5	7	5
	2022	4–5	6.5	9.2	7.6	6.9	1.2	16	9
	2022	7–50	6.5	7.7	6.9	6.8	0.4	6	8
The falling site of spherical fuel tanks (sampling depth 0–25 cm), *sampling distance from the fragments in m									
Water-soluble NO <sub>2</sub> <sup>-</sup> , mg/kg	2023	0–0.5	<1				–	–	5
	2023	10–25	<1	1.6	<1	<1	–	73	3
	2022	0–0.5	<1				–	–	8
	2022	4–5	<1	2.0	<1	<1	–	71	8
	2022	10–25	<1	3.2	<1	<1	–	96	19
Water-soluble NO <sub>3</sub> <sup>-</sup> , mg/kg	2023	0–0.5	<1	13.0	6.1	7.6	5.5	90	5
	2023	10–25	<1	47.0	16.9	3.2	26.1	154	3
	2022	0–0.5	<1	77.0	11.0	2.0	26.7	244	8
	2022	4–5	<1	26.0	8.0	1.7	11.3	142	8
	2022	10–25	<1	19.0	3.2	1.1	4.8	147	19
pH	2023	0–0.5	8.4	9.9	8.9	8.7	0.5	6	11
	2023	10–25	9.0	9.4	9.2	9.3	0.2	2	3
	2022	0–0.5	7.5	9.5	8.7	8.6	0.7	8	14
	2022	4–5	8.3	9.1	8.6	8.5	0.3	3	8
	2022	10–25	8.0	9.8	8.7	8.7	0.5	6	19
The falling site of spherical fuel tanks (sampling depth 25–50 cm), *sampling distance from the fragments in m									
Water-soluble NO <sub>2</sub> <sup>-</sup> , mg/kg	2023	0–0.5	<1	2.3	0.9	<1	0.8	94	5
	2023	10–25	<1	34	18	18	17	96	3
	2022	0–0.5	<1				–	–	8
	2022	4–5	<1				–	–	8
	2022	10–25	<1	3.2	0.7	0.5	0.6	93	19
Water-soluble NO <sub>3</sub> <sup>-</sup> , mg/kg	2023	0–0.5	1.1	32.0	8.1	1.5	13.4	166	5
	2023	10–25	<1	10.0	4.9	4.3	4.8	97	3
	2022	0–0.5	<1	11.0	3.9	2.1	4.4	114	8
	2022	4–5	<1	7.3	2.6	1.3	2.9	112	8
	2022	10–25	<1	18.0	2.7	1.2	4.1	152	19
pH	2023	0–0.5	8.1	8.9	8.6	8.6	0.3	3	7
	2023	10–25	8.5	8.9	8.7	8.8	0.2	2	3
	2022	0–0.5	7.6	9.3	8.4	8.4	0.6	7	10
	2022	4–5	7.1	8.7	8.2	8.4	0.5	6	8
	2022	10–25	7.0	8.5	8.1	8.2	0.4	5	19

**Table 2** (continued)

Soil property	Year	Sampling*	min	max	<i>M</i>	<i>Me</i>	<i>SD</i>	<i>Cv</i> , %	<i>n</i>
The falling site of spherical fuel tanks (sampling depth 50–100 cm), *sampling distance from the fragments in m									
Water-soluble NO <sub>2</sub> <sup>-</sup> , mg/kg	2023	0–0.5	<1	3.0	1.0	0.5	1.1	112	5
	2023	10–25	17	37	29	34	11	37	3
	2022	0–0.5	<1				–	–	8
	2022	4–5	<1	1.6	0.6	<1	0.4	61	8
	2022	10–25	<1	0.5	0.5	<1	0.0	0	19
Water-soluble NO <sub>3</sub> <sup>-</sup> , mg/kg	2023	0–0.5	<1	41	9	<1	18	202	5
	2023	10–25	<1	16	6	<1	9	158	3
	2022	0–0.5	<1	16.0	4.5	1.2	6.5	145	8
	2022	4–5	<1	12.0	3.7	1.1	5.2	141	8
	2022	10–25	<1	12.0	2.6	<1	3.5	134	19
pH	2023	0–0.5	7.9	8.4	8.1	8.2	0.2	3	7
	2023	10–25	8.5	8.8	8.6	8.6	0.2	2	3
	2022	0–0.5	6.8	9.1	7.8	7.6	0.8	10	10
	2022	4–5	6.7	7.9	7.5	7.6	0.4	5	8
	2022	10–25	6.7	8.0	7.3	7.3	0.4	6	19

*min* minimum, *max* maximum, *M* mean, *Me* median, *SD* standard deviation, *Cv* coefficient of variation, *n* number of samples

topsoil accumulate at the soil uppermost layer in the evaporate type of the geochemical barrier according to Perel'man (1967). By the end of spring, these chemicals are washed away (again to subsoil) by meltwater. The decrease in the concentration of easily soluble anions is compensated by an increase in the concentration of HCO<sub>3</sub><sup>-</sup>, formed during the dissolution of soil carbonates and air CO<sub>2</sub>.

The increased content of water-soluble NO<sub>3</sub><sup>-</sup> ( $p=0.147$ ) and NO<sub>2</sub><sup>-</sup> ( $p=0.003$ ) in the soil in spring is due to the active mineralization of plant residues that arrived on the soil surface in summer and autumn, since in September, the activity of the soil microbiota is still low and fresh mortmass is weakly transformed. This is confirmed by the increase in the spring concentration of total N ( $p=0.0007$ ), which accumulates in the soil due to the decomposition of mortmass. During the growing season, N compounds are actively absorbed by plants from the soil. By September relative to May in the soil, the concentration of these substances decreases.

## Second stage falling site

In the 0–25 cm topsoil layer at the second stage falling site, the pH value varied from 6.1 to 8.2 (Figs. 1 and 2) with minimum values in 2022. Such pH values are typical for Aridisols in Central and Eastern Asia (Kadono et al. 2008; Pankova and Gerasimova 2012; Salbu et al. 2013).

At the second stage falling site, the maximum content of TPHs reached 1645, 25, and 147 mg/kg in 2018, 2022, and 2023, respectively (Fig. 3). It is at least 4.9 times lower than the maximal permissible concentration proposed for light petroleum hydrocarbons, e.g., gasoline, kerosene, jet

fuel, and diesel in Aridisols (Pikovskii et al. 2003). Such concentration of TPHs corresponds to an initial load of pollutants as high as 5000 mg/kg according to the experiments conducted with Aridisols (Koroleva et al. 2024). In Aridisols, it decreased to safety level for soil microbiome and vegetation during a year. In addition, the proportion of samples containing TPHs > 5 mg/kg (lower limit of detection) decreased from 71 to 12 and 6%. That is, there is a natural self-purification of the soils from jet-fuel contamination.

According to the results of the paired Wilcoxon test, the content of TPHs in studied soils was higher in autumn than in spring ( $p=0.028$ ;  $n=24$ ). In autumn, 2 times more samples with the considerable concentration of TPHs (> 5 mg/kg) were found than in spring. Moreover, maximal detected values were higher in autumn than in spring and reached 155 and 12 mg/kg, respectively. This may be due to the migration of highly volatile hydrocarbons from the deep subsoil layers to the topsoil during June–October and their migration deep into the subsoil with meltwater. A similar situation was observed in the field experiments with jet-fuel spills in the Baikonur cosmodrome (Semenkov et al. 2023). It could be assumed that autumn is the most optimal time for monitoring the content of TPHs in soils because of identification of increased values of TPHs is more likely.

## Falling site of the spherical fuel tanks

In the 0–25 cm topsoil layer at the emergency falling site of the spherical fuel tanks, the pH value varied from 6.3 to 9.6 (Figs. 4 and 5) with minimum values in 2022. Observed

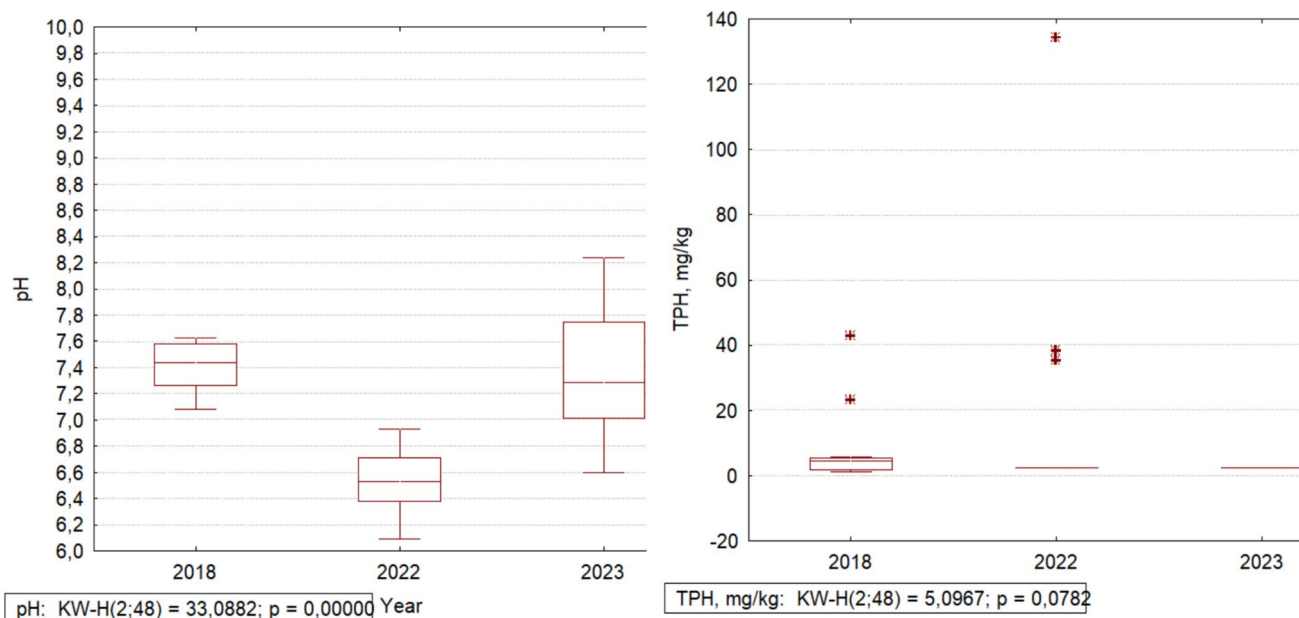


**Fig. 1** Dynamics of pH value and TPH content in the topsoil 0–25 cm layer at the second stage falling site according to data by the Infracos laboratory. Box, first and third quartiles. Whiskers, non-outlier range.

Circles, outliers. The horizontal line, mean. Asterisks, extremes. Below the graphs are the results of the Kruskal–Wallis *H*-test

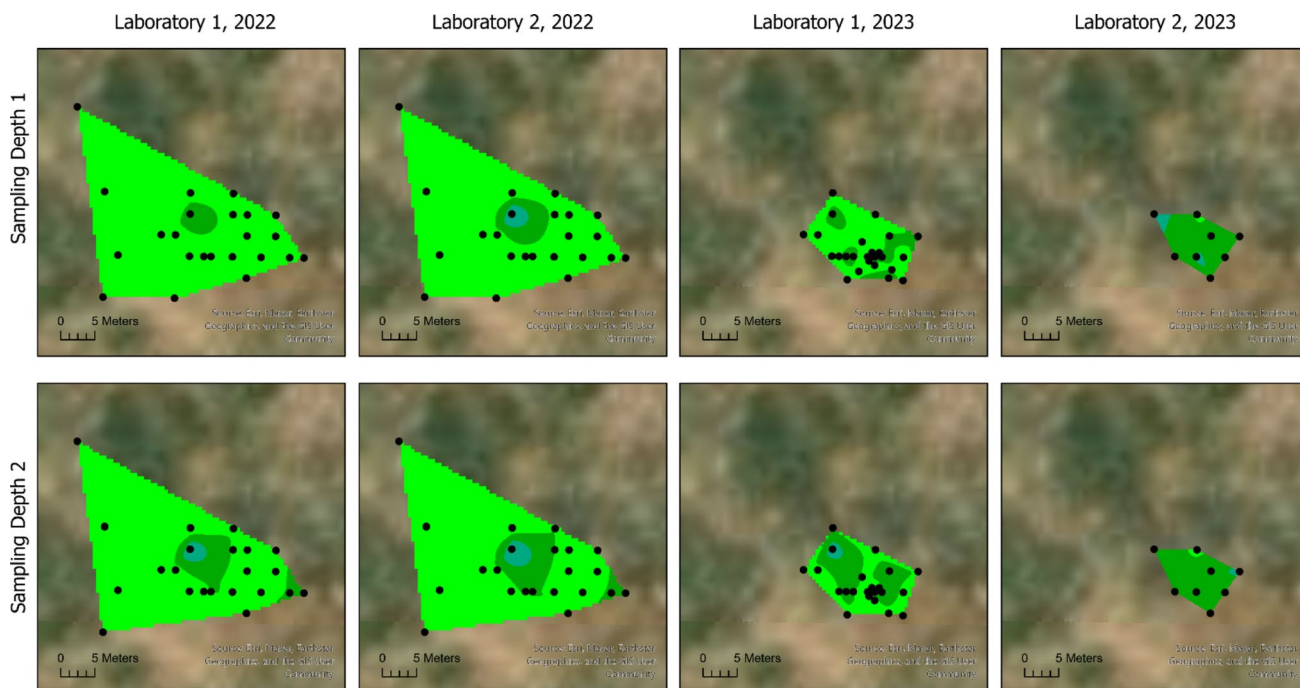


**Fig. 2** Spatial differentiation of pH in 0–25 cm (sampling depth 1) and 25–50 cm (sampling depth 2) of soils sampled at the second stage falling site according to data by the laboratories of the Yuzhny Space Center (Laboratory 1) and Infracos (Laboratory 2)

spatial differentiation of the pH value and the concentration of  $\text{NO}_3^-$  and  $\text{NO}_2^-$  (Figs. 6 and 7) is typical for Aridisols of Kazakhstan (Koroleva et al. 2021).

The maximum UDMH content detected at the falling site of the spherical fuel tanks reached 1.4 and 21.7 mg/kg in 2018 and 2019, respectively (Fig. 8), which is many times higher than the maximal permissible concentration

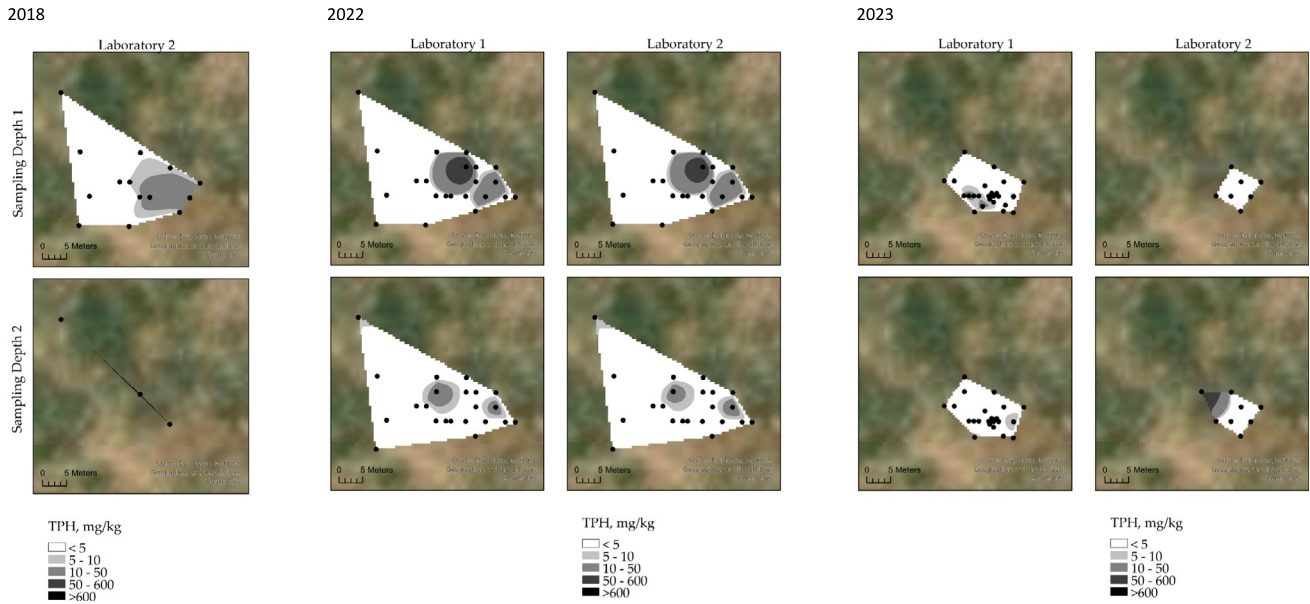


**Fig. 3** Spatial differentiation of the content of TPHs in sampling depth 1 (0–25 cm) and 2 (25–50 cm) of soils sampled at the second stage falling site according to data by the laboratories of Yuzhny space center (Laboratory 1) and Infracos (Laboratory 2) in 2018–2023

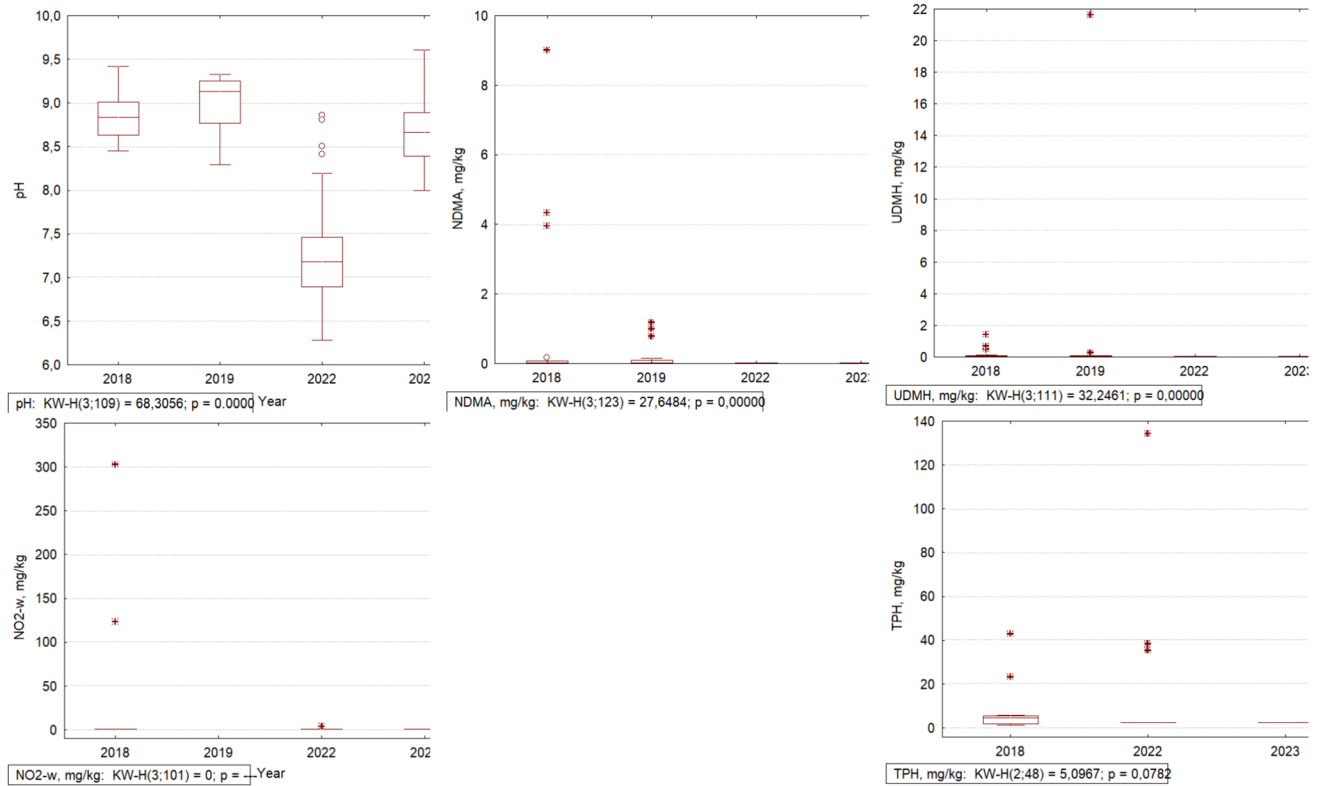


**Fig. 4** Dynamics of properties in the 0–25 cm topsoil layer at the falling site of the spherical fuel tanks according to the data by the Infracos laboratory. Box, first and third quartiles. Whiskers, non-

outlier range. Circles, outliers. The horizontal line, mean. Asterisks, extremes. Below the graphs are the results of the Kruskal–Wallis *H*-test

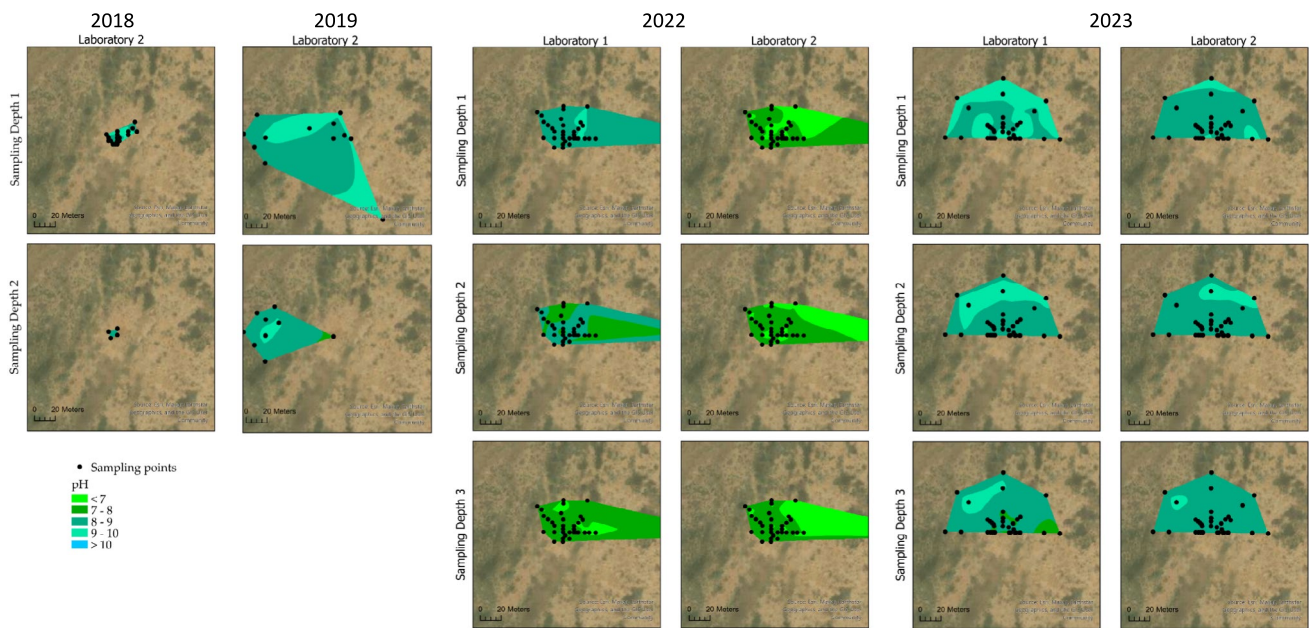


**Fig. 5** Dynamics of the pH value in the 0–25 (sampling depth 1), 25–50 (sampling depth 2), and 50–100 (sampling depth 3) cm soil layers at the falling site of the spherical fuel tanks according to the data by the laboratories of Yuzhny Space Center (1) and Infracos (2) in 2018–2023

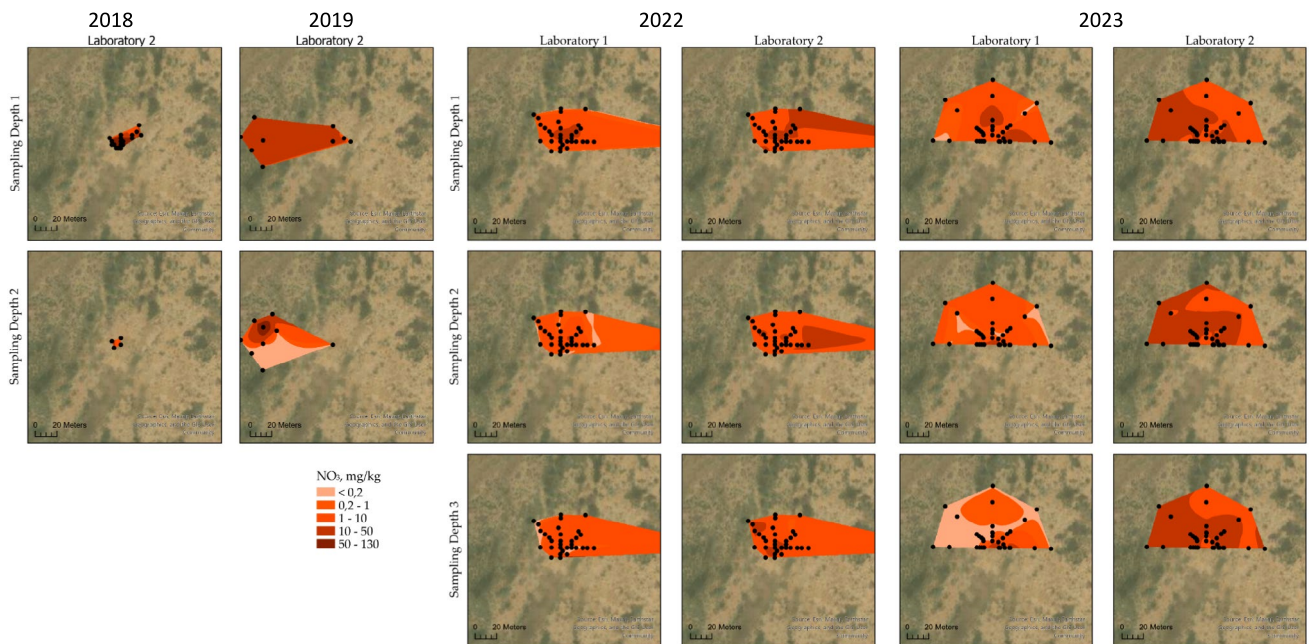


**Fig. 6** Dynamics of  $\text{NO}_3^-$  concentration in the 0–25 (sampling depth 1), 25–50 (sampling depth 2), and 50–100 (sampling depth 3) cm soil layers at the falling site of the spherical fuel tanks according to the

data by the laboratories of Yuzhny Space Center (1) and Infracos (2) in 2018–2023

for soils in Kazakhstan (Koroleva et al. 2023). High concentrations were also characteristic of NDMA as one of the main derivatives of UDMH (Kosyakov et al. 2019; Ul’yanovskii et al. 2020; Koroleva et al. 2023): 9.0 and 1.2 mg/kg in 2018 and 2019, respectively. After the

removal of the polluted soils, the values for both chemicals returned to normal.

In 2022 and 2023, the content of NDMA and UDMH was below the detection limit of the highly selective analysis method used—0.05 mg/kg—in all analyzed soil samples

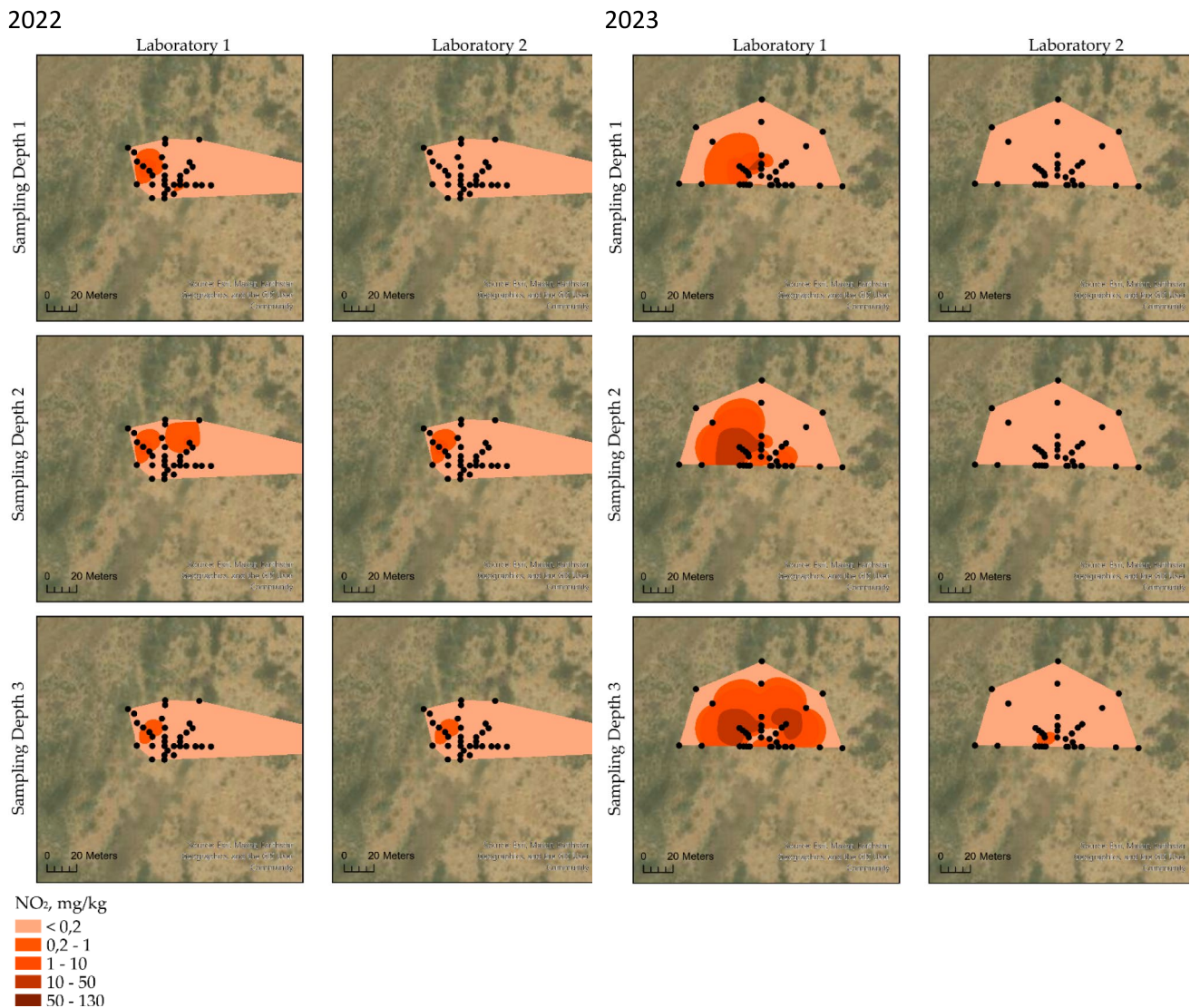


**Fig. 7** Dynamics of NO<sub>2</sub><sup>-</sup> concentration in the 0–25 (sampling depth 1), 25–50 (sampling depth 2), and 50–100 (sampling depth 3) cm soil layers at the falling site of the spherical fuel tanks according to the

data by the laboratories of Yuzhny Space Center (1) and Infracos (2) in 2022–2023

( $n = 144$ ), which reflects the high efficiency of the implemented remediation in the emergency falling site.

Success in analytical diagnostics of organic substances, in particular UDMH derivatives (Sholokhova et al. 2022; Hu et al. 2022; Karnaeva et al. 2022; Milyushkin and Karnaeva 2023), suggests the existence of about 300 UDMH derivatives (Kosyakov et al. 2019; Wang et al. 2021), of which only 13 compounds have been reliably identified so far (Smolenkov et al. 2005; Rodin et al. 2008, 2012). The impact of these derivatives on human health, living organisms, and ecosystems has not yet been reliably assessed (Slonim 1977; Smolenkov et al. 2013). Some authors claim higher toxicity of derivatives in comparison with the

initial substance (Slonim 1977; Ivanova et al. 2023). Others inform that UDMH is more toxic than its derivatives (Rogers and Back 1981; Smolenkov et al. 2005, 2013; Rodin et al. 2008, 2012).

This limits the possibility of justifying maximum permissible concentrations of UDMH transformation products in the environment. At present, in Russia and the Republic of Kazakhstan, among all UDMH derivatives, the maximum permissible concentration in soil is justified only for NDMA. Therefore, only concentrations of UDMH and NDMA can be used as criteria for the degree of soil pollution at launch vehicle emergency falling sites in the context of damage assessment. Toxicity and carcinogenicity of NDMA are

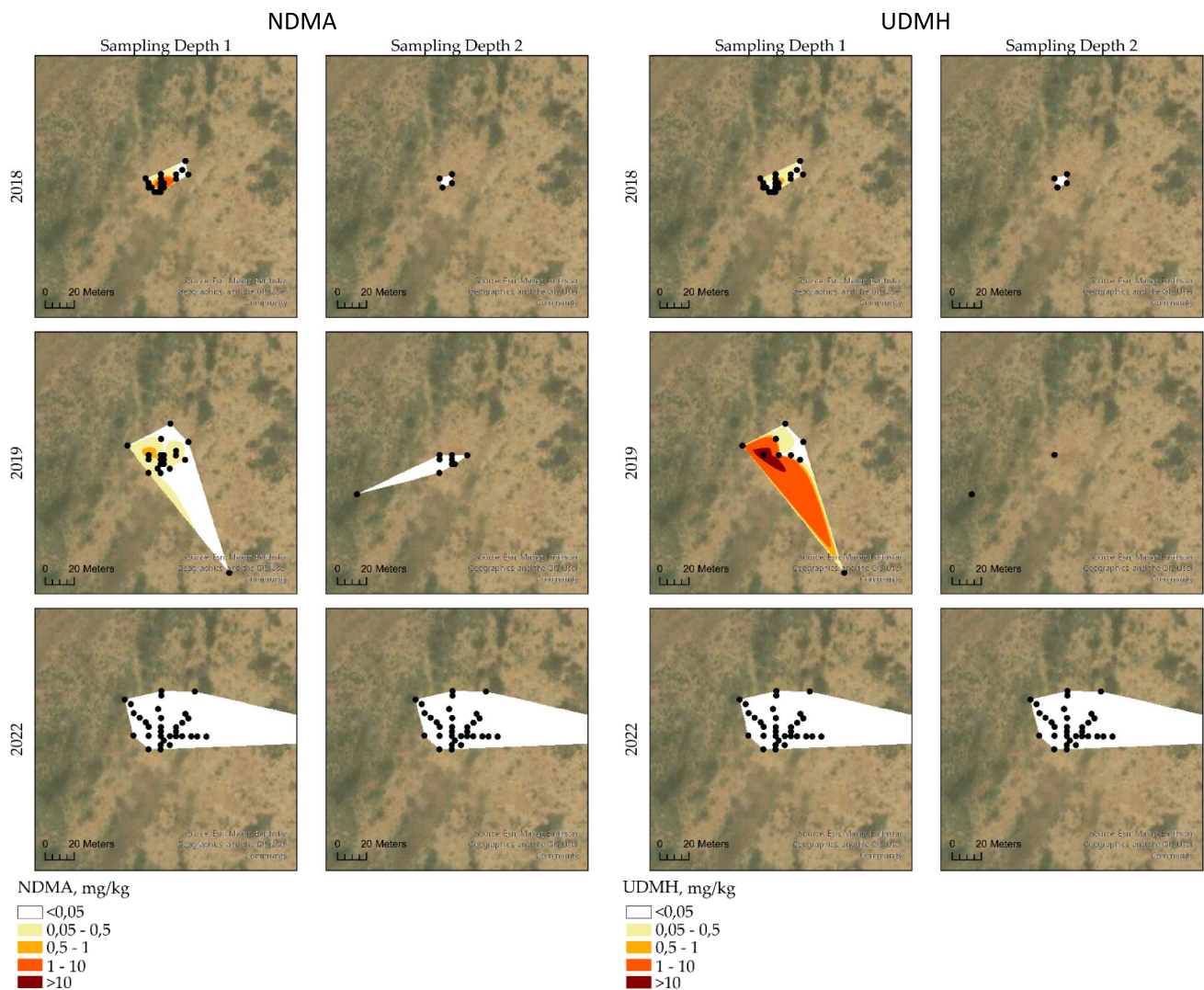


**Fig. 8** Dynamics of NDMA and UDMH concentrations in the 0–25 (sampling depth 1) and 25–50 (sampling depth 2) cm soil layers at the falling site of the spherical fuel tanks according to the data by the Infracos laboratory in 2018–2023

undoubtedly (Carter 1974; Nguyen et al. 2021). However, its detection in drugs, drinking water, food, and cosmetics—which were not in contact with UDMH—indicates that this substance is not a reliable indicator of UDMH pollution (Koroleva et al. 2023).

### Whole data set

Among the data set for samples collected at the same points, attention is drawn to the lack of significant correlation between the values obtained in autumn and spring for the vast majority of studied soil properties (Table S3). The exception is the pH value and the content of water-soluble  $\text{NO}_2^-$ , for which a direct relationship was obtained between the levels found in different seasons of the year at the same points. The content of water-soluble  $\text{Cl}^-$  was minimal in

spring at points where maximum concentrations were observed in autumn. Perhaps this is due to the predominant downward movement of  $\text{Cl}^-$  in microdepressions, where salts are precipitated in the evaporate type of the geochemical barrier during summer. Observed differentiation indirectly confirms the fact that in different seasons of the year, soils can be classified as Solonchaks during summer and autumn due to high salinity in the topsoil or as Solonetz or Gypsisols in spring due to low salinity in the topsoil.

Despite the smaller data subset for samples collected in the fall of 2022 (Table S 4) and in the spring of 2023 (Table S 5), a more definite correlation was obtained, which is associated with an increase in the degree of homogeneity of the sample and the elimination of the contribution of seasonal variability in the values of soil properties. Thus, the content of exchangeable  $\text{Ca}^{2+}$  determines the absolute majority

(> 80%) of the variance in the CEC. Moreover, this very close connection remains in both spring and autumn. The pH value is determined primarily by the basicity of  $\text{CO}_3^{2-}$ . A stable close relationship was also revealed between the content of easily soluble anions ( $\text{SO}_4^{2-}$  and  $\text{Cl}^-$ ), in the absence of significant relationship with the content of  $\text{HCO}_3^-$  and  $\text{CO}_3^{2-}$ . Significant correlations were not found between cations and anions, which reflects more active downward movement of negatively charged ions relative to positively charged ions which are absorbed by soil colloids. This may indicate the possibility of solonetzization of the soils under consideration.

### Comparison of soil properties in background and disturbed areas

At the second stage falling site, the soils significantly differ from the selected background soils (outside the zone of influence of accident-related factors) in pH value (Table S 6). It is due to the local peculiarities of the two compared territories and is not the fact of contamination, since the properties of soils at different distances from the fragments differ very little, even if we take a distance of 7–50 m, where no chemical contamination was recorded. There are only 3 exceptions, but they are not reproduced in another sampling season or insignificance after the Holm-Bonferroni correction.

For other key sites, it also turned out that they differ significantly from the background areas (outside the impact zone) in pH value (Table S 7). Key sites do not differ in the content of TPHs. In terms of the content of exchangeable  $\text{Ca}^{2+}$  and CEC, a reproducible picture is observed according to the data obtained from the cross-sections. At the second stage falling site, the content of exchangeable  $\text{Ca}^{2+}$  is lower relative to the background territories (median varies between 6–7 and 12–13 mmol/100 g in spring and autumn, respectively) and CEC (median 20 and 36 mmol/100 g varies slightly depending on the sampling season). In terms of the content of water-soluble  $\text{Cl}^-$ , the cross-sections at the second stage falling site and at the spherical fuel tanks differ significantly: in the autumn of 2022, there are more chlorides at the spherical fuel tanks falling site (14.2 g/kg versus 0.83 g/kg). In May of 2023, the opposite situation was observed (0.5 and 102 mg/kg), which was due to more active migration of salts in more moist mesodepressions. Salt leaching from the topsoil horizons due to the influence of rainwater or melted snow water was previously reported for diverse Aridisols (Li et al. 2024). There are no clear differences in other soil properties.

The pH values; the content of water-soluble  $\text{SO}_4^{2-}$ ,  $\text{Cl}^-$ , and  $\text{NO}_3^-$ ; and exchangeable  $\text{Ca}^{2+}$  and  $\text{Mg}^{2+}$ , TOC, Ntot, CEC, and basicity of carbonates and soda were within the

levels characteristic of background soils in Kazakhstan (Koroleva et al. 2021).

### Conclusion

The emergency falling of the Soyuz launch vehicle on 11.10.2018 resulted in the formation of several falling sites:

- Four regular falling sites of the first stage in the initially specified territory.
- Fairing falling site in the unspecified falling region. Here, soils were not contaminated with rocket propellants.
- The second stage falling site in the unspecified falling region. Here, jet fuel spilled at 400 m<sup>2</sup>. The maximal concentration of jet fuel reached 1645 mg/kg and decreased to the background level during 3.5 years.
- The third stage is destroyed after detonation in the atmosphere scattered at the territory of 4.4 km<sup>2</sup> outside any falling region. Falling sites were not formed due to the small size of fragments.
- The falling site of the spherical fuel tanks outside any falling region. Here, the spillage of highly toxic carcinogenic UDMH was found at the territory of 9 m<sup>2</sup>. The concentration of highly toxic UDMH and NDMA reached 21.7 and 9.0 mg/kg, respectively. Moreover, vegetation burnt out at 950 m<sup>2</sup>.

It should be highlighted that the falling site of the System for Emergency Rescue (i.e., abort mode) was not formed because it had pulled the landing module holding the cosmonauts free of the rocket and landed softly.

The presented materials can be used to optimize the restoration of disturbed arid ecosystems and future monitoring work at sites of regular landing of the first stages and emergency crash sites of launch vehicles. Obtained results can be used in the life cycle assessment of space transportation.

**Supplementary Information** The online version contains supplementary material available at <https://doi.org/10.1007/s11356-025-35889-4>.

**Acknowledgements** Chemical-analytical work was carried out in accredited laboratories of the Republican State Enterprise Infracos (Almaty, Kazakhstan) and Yuzhny Space Center (Baikonur, Kazakhstan). The authors are grateful to all who participated in the field and laboratory works.

**Author contribution** I.S.: conceptualization, data curation, formal analysis, investigation (fieldwork), methodology, validation, visualization, writing—original draft preparation, review and editing. Ye.B.: conceptualization, funding acquisition, investigation (fieldwork), methodology, resources, writing—review and editing. Ye.S.: data curation, validation, writing—review and editing. A.K.: software, visualization. S.L.: investigation (fieldwork), writing—review and editing.

G.K.: writing—review and editing. Ye.Ye.: investigation (fieldwork), data curation. A.B.: investigation (fieldwork), validation. T.K.: conceptualization, methodology, supervision, writing—review and editing. All authors have read and agreed to the published version of the manuscript.

**Funding** This research was funded by the Joint Work Program for Integrated Environmental and Socio-Hygienic Monitoring of Areas Affected by the Emergency Crash of the Soyuz-FG Launch Vehicle with the Soyuz MS-10 Transport Manned Spacecraft on October 11, 2018, to 2021–2023.

**Data availability** The experimental data that support the findings of this study are available in Mendeley with the identifier <https://data.mendeley.com/datasets/47twnk5dsh/1> (Bekeshev et al. 2024).

## Declarations

**Ethical approval** Not applicable.

**Consent to participate** Not applicable.

**Consent for publication** Not applicable.

**Competing interests** Not applicable.

## References

- Bekeshev Y, Semenov I, Stepanova Y et al (2024) Data on the temporal changes in soil properties at the emergency crash site of the launch vehicle ‘Soyuz-FG’ in Kazakhstan. *Data Br* 55:110646. <https://doi.org/10.1016/j.dib.2024.110646>
- Bolotnik TA, Smolenkov AD, Smirnov RS, Shpigun OA (2015) Determination of rocket kerosene in soil by static headspace analysis coupled with gas chromatography–mass spectrometry. *Moscow Univ Chem Bull* 70:168–174. <https://doi.org/10.3103/S0027131415040021>
- Bolotnik TA, Plyushchenko IV, Smolenkov AD et al (2018) Identification of spillages of semi-volatile hydrocarbon fuels in soils by gas chromatography–mass spectrometry. *J Anal Chem* 73:570–575. <https://doi.org/10.1134/S1061934818060035>
- Carter R (1974) IARC Monographs: The Evaluation of Carcinogenic Risk of Chemicals to Man. Volume 4: Some Aromatic Amines, Hydrazine and Related Substances, N-Nitroso Compounds and Miscellaneous Alkylating Agents, Volume 5: Some Organochlorine Pesticides, Assessment of the Carcinogenicity and Mutagenicity of Chemicals: Report of a WHO Scientific Group. *J Clin Pathol* 27:926–926. <https://doi.org/10.1136/jcp.27.11.926>
- Dallas JA, Raval S, Alvarez Gaitan JP et al (2020) The environmental impact of emissions from space launches: a comprehensive review. *J Clean Prod* 255:120209. <https://doi.org/10.1016/j.jclepro.2020.120209>
- Epifanov IK, Kondratyev AD, Doroshina SV (2009) Environmental damage in result of ascent-phase abort of rocket carriers. *Natzional’nye Interes Priorityety i Bezop* 24:53–57
- Gennadiev AN, Pikovskii YI, Zhidkin AP et al (2015) Factors and features of the hydrocarbon status of soils. *Eurasian Soil Sci* 48:1193–1206. <https://doi.org/10.1134/S1064229315110071>
- Gooijer C, Kozin I, Velthorst NH (1997) Shpol’skii spectrometry, a distinct method in environmental analysis. *Mikrochim Acta* 127:149–182. <https://doi.org/10.1007/BF01242719>
- Hu C, Zhang Y, Zhou Y et al (2022) Unsymmetrical dimethylhydrazine and related compounds in the environment: recent updates on pretreatment, analysis, and removal techniques. *J Hazard Mater* 432:128708. <https://doi.org/10.1016/j.jhazmat.2022.128708>
- Ivanova E, Osipova M, Vasilieva T et al (2023) The recycling of sub-standard rocket fuel n, n-dimethylhydrazine via the involvement of its hydrazones derived from glyoxal, acrolein, metacrolein, crotonaldehyde, and formaldehyde in organic synthesis. *Int J Mol Sci* 24:17196. <https://doi.org/10.3390/ijms242417196>
- Kadono A, Funakawa S, Kosaki T (2008) Factors controlling mineralization of soil organic matter in the Eurasian steppe. *Soil Biol Biochem*. <https://doi.org/10.1016/j.soilbio.2007.11.015>
- Karnaeva AE, Milyushkin AL, Khesina ZB, Buryak AK (2022) 1-Methyl-1H-1,2,4-triazole as the main marker of 1,1-dimethylhydrazine exposure in plants. *Environ Sci Pollut Res* 29:64225–64231. <https://doi.org/10.1007/s11356-022-22157-y>
- Kopack RA (2019) Rocket wastelands in Kazakhstan: scientific authoritarianism and the Baikonur cosmodrome. *Ann Am Assoc Geogr* 109:556–567. <https://doi.org/10.1080/24694452.2018.1507817>
- Kopack R (2021) Baikonur 2.0: ‘inland-offshore’ space economies in post-Soviet Kazakhstan. *Cult Theory Crit* 62:96–112. <https://doi.org/10.1080/14735784.2021.1929363>
- Koroleva TV, Semenov IN, Sharapova AV et al (2021) Ecological consequences of space rocket accidents in Kazakhstan between 1999 and 2018. *Environ Pollut* 268:115711. <https://doi.org/10.1016/j.envpol.2020.115711>
- Koroleva TV, Semenov IN, Lednev SA, Soldatova OS (2023) Unsymmetrical dimethylhydrazine (UDMH) and its transformation products in soils: a review of the sources, detection, behavior, toxicity, and remediation of polluted territories. *Eurasian Soil Sci* 56:210–225. <https://doi.org/10.1134/S1064229322602001>
- Koroleva TV, Semenov IN, Lednev SA, Soldatova OS (2024) Jet fuel as a source of soil pollution: a review. *Eurasian Soil Sci* 57:1519–1524. <https://doi.org/10.1134/S1064229324601264>
- Kosyakov DS, Ul’yanovskii NV, Pikovskoi II et al (2019) Effects of oxidant and catalyst on the transformation products of rocket fuel 1,1-dimethylhydrazine in water and soil. *Chemosphere* 228:335–344. <https://doi.org/10.1016/j.chemosphere.2019.04.141>
- Li W, Li J, Wu Y et al (2024) Soil organic matter and bulk density: driving factors in the vegetation-mediated restoration of coastal saline lands in North China. *Agron* 14(9):2007. <https://doi.org/10.3390/agronomy14092007>
- Liu L, Jia P, Huang Y et al (2022) Space industrialization. *Environ Chem Lett* 21:5571. <https://doi.org/10.1007/s10311-022-01411-2>
- Maksimov AV (2020) Accidents of soviet launch vehicles. *astro.websib.ru/kosmo/sprav/avaria*. Accessed 10 Jan 2020
- Meira M, Quintella CM, Tanajura ADS et al (2011) Determination of the oxidation stability of biodiesel and oils by spectrofluorimetry and multivariate calibration. *Talanta* 85:430–434. <https://doi.org/10.1016/j.talanta.2011.04.002>
- Milyushkin AL, Karnaeva AE (2023) Unsymmetrical dimethylhydrazine transformation products: a review. *Sci Total Environ* 891:164367. <https://doi.org/10.1016/j.scitotenv.2023.164367>
- Nguyen HN, Chenoweth JA, Beberta VS et al (2021) The toxicity, pathophysiology, and treatment of acute hydrazine propellant exposure: a systematic review. *Mil Med* 186:e319–e326. <https://doi.org/10.1093/milmed/usaa429>
- Pankova EI, Gerasimova MI (2012) Desert soils: properties, pedogenic processes, and classification. *Arid Ecosyst*. <https://doi.org/10.1134/S2079096112020084>
- Pansu M, Gautheyrou J (2006) Handbook of Soil Analysis. <https://doi.org/10.1007/978-3-540-31211-6>
- Patra D, Mishra AK (2000) Effect of sample geometry on synchronous fluorimetric analysis of petrol, diesel, kerosene and their mixtures at higher concentration. *Analyst* 125:1383–1386. <https://doi.org/10.1039/b003876h>

- Perel'man AI (1967) *Geochemistry of epigenesis*, 1st edn. Springer, Boston
- Pikovskii YI, Gennadiev AN, Chernyanskii SS, Sakharov GN (2003) The problem of diagnostics and standardization of the levels of soil pollution by oil and oil products. *Eurasian Soil Sci* 36:1010–1017
- Pikovskii YI, Korotkov LA, Smirnova MA, Kovach RG (2017) Laboratory analytical methods for the determination of the hydrocarbon status of soils (a review). *Eurasian Soil Sci* 50:1125–1137. <https://doi.org/10.1134/S1064229317100076>
- Ponomarenko SA, Smolenkov AD, Shpigun OA (2009) Determination of 1,1-dimethylhydrazine and its decomposition products using ion-pair chromatography. *Moscow Univ Chem Bull.* <https://doi.org/10.3103/S0027131409030079>
- Rodin IA, Moskvina DN, Smolenkov AD, Shpigun OA (2008) Transformations of asymmetric dimethylhydrazine in soils. *Russ J Phys Chem A* 82:911–915. <https://doi.org/10.1134/S003602440806006X>
- Rodin IA, Smirnov RS, Smolenkov AD et al (2012) Transformation of unsymmetrical dimethylhydrazine in soils. *Eurasian Soil Sci* 45:386–391. <https://doi.org/10.1134/S1064229312040096>
- Rogers AM, Back KC (1981) Comparative mutagenicity of hydrazine and 3 methylated derivatives in L5178Y mouse lymphoma cells. *Mutat Res Toxicol* 89:321–328. [https://doi.org/10.1016/0165-1218\(81\)90113-0](https://doi.org/10.1016/0165-1218(81)90113-0)
- Salbu B, Burkitbaev M, Strømman G et al (2013) Environmental impact assessment of radionuclides and trace elements at the Kurday U mining site, Kazakhstan. *J Environ Radioact.* <https://doi.org/10.1016/j.jenvrad.2012.05.001>
- Semenkov IN, Shelyakin PV, Nikolaeva DD et al (2023) Data on the temporal changes in soil properties and microbiome composition after a jet-fuel contamination during the pot and field experiments. *Data Br* 46:108860. <https://doi.org/10.1016/j.dib.2022.108860>
- Sholokhova AY, Grinevich OI, Matyushin DD, Buryak AK (2022) Machine learning-assisted non-target analysis of a highly complex mixture of possible toxic unsymmetrical dimethylhydrazine transformation products with chromatography-mass spectrometry. *Chemosphere* 301:135764. <https://doi.org/10.1016/j.chemosphere.2022.135764>
- Slonim AR (1977) Acute toxicity of selected hydrazines to the common guppy. *Water Res* 11:889–895. [https://doi.org/10.1016/0043-1354\(77\)90077-X](https://doi.org/10.1016/0043-1354(77)90077-X)
- Smolenkov AD, Krechetov PP, Pirogov AV et al (2005) Ion chromatography as a tool for the investigation of unsymmetrical hydrazine degradation in soils. *Int J Environ Anal Chem* 85:1089–1100. <https://doi.org/10.1080/03067310500191454>
- Smolenkov AD, Poputnikova AT, Smirnov RS et al (2013) Comparative assessment of toxicity of unsymmetrical dimethyl hydrazine and its decomposition products by bioassay methods. *Theor Appl Ecol* 2:85–90
- Ul'yanovskii NV, Lakhmanov DE, Pikovskoi II et al (2020) Data on the spatial distribution of 1,1-dimethylhydrazine and its transformation products in peat bog soil of rocket stage fall site in Russian North. *Data Br* 30:105614. <https://doi.org/10.1016/j.dib.2020.105614>
- UNDP (2004) *Environment and development nexus in Kazakhstan*. Almaty
- Wang H, Jia Y, Jing G, Wu X (2021) A novel toxicity prediction model for hydrazine compounds based on 1D–3D molecular descriptors. *Comput Toxicol* 18:100169. <https://doi.org/10.1016/j.comtox.2021.100169>
- Williams A (2013) Proton-M crash adds to Russian rocket woes. *New Sci* 219:5. [https://doi.org/10.1016/S0262-4079\(13\)61649-8](https://doi.org/10.1016/S0262-4079(13)61649-8)
- Włodarski M, Bombalska A, Mularczyk-Oliwa M et al (2013) Fluorimetric techniques in analysis and classification of fuels. In: *Laser technology 2012: Applications of lasers*

**Publisher's Note** Springer Nature remains neutral with regard to jurisdictional claims in published maps and institutional affiliations.

Springer Nature or its licensor (e.g. a society or other partner) holds exclusive rights to this article under a publishing agreement with the author(s) or other rightsholder(s); author self-archiving of the accepted manuscript version of this article is solely governed by the terms of such publishing agreement and applicable law.